Biogeosciences, 11, 1125–1136, 2014
www.biogeosciences.net/11/1125/2014/
doi:10.5194/bg-11-1125-2014

Biogeosciences Open Access

Authigenic phase formation and microbial activity control Zr, Hf, and rare earth element distributions in deep-sea brine sediments

P. Censi[1,2], F. Saiano[3], P. Zuddas[4], A. Nicosia[2], S. Mazzola[2], and M. Raso[1]

[1]DISTEM Department, University of Palermo, Via Archirafi, 22 90123 Palermo, Italy
[2]IAMC-CNR, UOS Capo Granitola, via del Mare, 3, 91021 Campobello di Mazara, Italy
[3]SAF Department, University of Palermo, Viale delle Scienze, 13, 90128 Palermo, Italy
[4]Institute des Sciences de la Terre de Paris, UPMC-Sorbonne Universités 4, place Jussieu 75005 Paris, France

Correspondence to: P. Censi (paolo.censi@unipa.it)

Received: 3 April 2013 – Published in Biogeosciences Discuss.: 31 May 2013
Revised: 27 December 2013 – Accepted: 6 January 2014 – Published: 26 February 2014

Abstract. Sediments collected from hypersaline and anoxic deep-sea basins in the eastern Mediterranean (Thetis, Kryos, Medee, and Tyro) were characterised in terms of their mineralogical composition, the distributions of rare earth elements (REE), Zr, and Hf and their content of microbial DNA. We identified two major mineralogical fractions: one fraction of detritic origin was composed of quartz, gypsum, and low-Mg calcite bioclasts (with $0 < \mathrm{Mg} < 0.07\,\%$) and another fraction of authigenic origin constituted of halite, dolomite, high-Mg calcite (with a Mg content of up to 22 %) and rare bischofite and showed a textural evidence of microbial assemblages.

We found that in the Medee and Tyro sediments, the shale-normalised REE pattern of these sediments is strongly enriched in middle REE (MREE), whereas in the Thetis and Tyro basins, a positive Gd anomaly in the residue was obtained after the removal of the water-soluble fraction. In all investigated basins, Y / Ho ratio clustered around chondritic values, whereas Zr / Hf ratio ranged from slightly subchondritic to superchondritic values. Subchondritic Y / Ho and Zr / Hf values were mainly found in the high-Mg carbonate having a microbial origin. The observed preferential removal of Zr with respect to Hf without significant partitioning of Y with respect to Ho indicates that the Zr / Hf ratio and Y–Ho fractionations are influenced by the microbial activity in the sediments. We propose that the concurrent Y-Ho and Zr–Hf fractionations are a suitable tracer of microbial activity in marine sediments.

1 Introduction

The growing interest in rare earth elements (REE – lanthanides and yttrium, but not including scandium) Zr and Hf distributions in marine sediments started with the increased exploitation of these elements in several industrial practices (Andrianov et al., 2011; Du and Graedel, 2013; Moriwaki et al., 2013; Hein et al., 2013, and references therein). Several studies carried out during the last 25 yr have identified the processes responsible for REE adsorption onto the surface of Fe–Mn crusts in marine environments (Bau and Koschinsky, 2009, and reported references), but few have focused on processes occurring during the crystallisation of authigenic minerals (Bach et al., 2003; Moller and Dulski, 1983; Himmler et al., 2010; Azmy et al., 2011; Ehya, 2012). There is a paucity of knowledge regarding processes affecting REE, Zr, and Hf distributions during carbonate crystallisation and their soluble salts in natural systems, and only limited number of studies have been carried out under laboratory conditions (Rimstidt et al., 1998; Pokrovsky et al., 1999). The difficulty in recognising these distributions when studying marine sediments is related to the occurrence of a wide spectrum of detritic minerals associated with authigenic phases such as Mg-rich calcite, dolomite, and soluble salts. The identification of processes allowing the accumulation of REE, Zr, and Hf in natural sedimentary assemblages requires a detailed knowledge of the mineralogical composition of the assemblage as well as the identification of microbial activity. Censi et al. (2013) recently demonstrated the capability of microbial assemblages to influence distributions of REE, Zr, and

Hf at the sediment–water interface in natural systems, previously shown under controlled lab conditions (Takahashi et al., 2005, 2007, 2010; Morikawi et al., 2013.

In this work, sediments collected from hypersaline deep-sea lakes located in the eastern Mediterranean Sea were investigated for effects related to the concurrent presence of detritic and authigenic minerals as well as microbial activity on REE distribution. These lakes occur in depressed areas of the eastern Mediterranean seafloor which are filled by hypersaline brines underlying the oxic water column (Cita, 2006, and references therein). These lakes are likely formed by dissolution of Messinian evaporites in addition to the reactions of authigenic Mg-rich carbonates and chlorine salts. These minerals are generally associated with detritic material accumulated during slumping episodes from seafloor elevations (Rimoldi and Cita, 2007). In the present study, the mineralogical composition of sedimentary assemblages was identified and the extent of microbial activity as well as REE, Zr, and Hf distribution were analysed to evaluate the geochemical behaviour of these elements in this complex environment where both inorganic and biological interfaces are active.

2 Materials and methods

Sediments from the eastern Mediterranean Sea during were collected during the 2010 MAMBA oceanic expedition using the RV *Urania* by M. Yakimov's team from the Italian National Research Council, Institute of Marine and Coastal Environment (IAMC), section of Messina (Italy). Sample collection was carried out on the seafloor of hypersaline lakes in the Medee, Tyro, Thetis, and Kryos basins in the eastern Mediterranean Sea near Crete (Fig. 1). These basins are located in the inner portion of the so-called "Mediterranean ridge accretionary complex" (Bortoluzzi et al., 2011) in the eastern basin. In this basin the Messinian evaporites are often located immediately below thin hemipelagic sediments (Ryan et al., 1973; Hsu et al., 1978). According to Camerlenghi (1990), tectonic deformation of seafloor sediments coupled with the submarine dissolution of Messinian evaporitic sediments (Cita, 2006) allowed for the formation of the basins and related hypersaline lakes formed therein.

Sediments were collected using an USGS-modified NEL box corer (Tranchida et al., 2011) and samples were stored in polyethylene liners at −20 °C until chemical analysis. In the laboratory, the defrosted cores were cut at 1–2 cm intervals and dried at 50 °C. Samples from the Thetis and Kryos basins were ultrasonically cleaned in high-purity water (resistivity at 25 °C = 18.2 $M\Omega\,cm^{-1}$) in order to remove salt minerals, while samples from the Tyro and Medee basins were analysed without further manipulations.

X-Ray investigations were carried out using a Philips PW14 1373 X-ray spectrometer using Cu-Kα radiation (2Θ range 3–90°, step size 0.02°, and a 1 min step time) and analysed by the Rietveld method (program: DiffracPlus TOPAS®, version 4.0; Bruker AXS Inc., Karlsruhe, Germany) using parameters for the Rietveld refinement method obtained from the Inorganic Crystal Structure Database (ICSD) database. This method consists of fitting the experimental XRD spectrum to the theoretical spectrum calculated by means of several structural parameters by the least-squares method refinement (Young, 1993). $MgCO_3$ content calculations were carried out according to the method reported by Zhang et al. (2012).

For analysis of the sediment textures, scanning electron microscopy (SEM) was used. Sediments, previously dried at 105 °C, were coarsely crushed in an agate mortar, mounted on aluminium stubs and carbon-coated. SEM analyses were carried out using a LEO 440 SEM equipped with an EDS system OXFORD ISIS Link and Si (Li) PENTAFET detector.

Chemical analyses were carried out by digesting 100 mg of each sample in 10 mL of a 1 : 1 HNO_3–H_2O_2 mixture in a sealed Teflon TFM bomb using a microwave mineraliser (CEM MARS 5 device). For Thetis and Kryos samples, the trace element composition was measured after removing the fraction of water-soluble salts (hereafter referred to as FWSS), while the entire sediment composition (hereafter called WS) of the Medee and Tyro samples was analysed. The WS sediment fractions were assumed to be representative of dissolved carbonates, sulfates, sulfides, and organic matter (being soluble in $HNO_3 : H_2O_2$ mixture), whereas silicate residue were separated from the dissolved phase after filtration onto previously acid-cleaned 0.45 µm Millipore™ filters. The filtered solution was diluted to 50 mL and stored for chemical analyses.

All chemical analyses were carried out by inductively coupled plasma mass spectrometry (ICP-MS) using an Agilent Technologies 7500ce series spectrometer equipped with a collision cell. The instrumental parameters were optimised daily using a 1 $ng\,mL^{-1}$ solution of ^{7}Li, ^{89}Y, ^{140}Ce, and ^{205}Tl, while maximum instrument sensitivity was tuned using ^{89}Y, each solution measured in triplicate. ICP-MS analyses were carried out with a classical external calibration approach which involved investigating a range of concentrations (between 2.5 and 500 $pg\,mL^{-1}$) for each element and using ^{205}Tl (1 $ng\,mL^{-1}$) as an internal standard to compensate for signal instability or sensitivity changes during the analysis. A 1 M HCl washing solution was run during the analysis to ensure that the memory effect, which was due to the more refractory elements, was negligible. Analyses were carried out in external calibration with standard solutions prepared daily by stepwise dilution of multi-element stock standard solutions from CPI International™ (1000 ± 5 $\mu g\,mL^{-1}$) in HCl medium.

The precision and accuracy of chemical data were evaluated by comparison to the USGS standard reference materials AGV-1 (andesite) and MAG (marine mud) in which the REE, Zr, and Hf concentrations were known and certified. The standard reference materials (about 0.2 g of solid powder) were digested in 12 mL of freshly prepared aqua

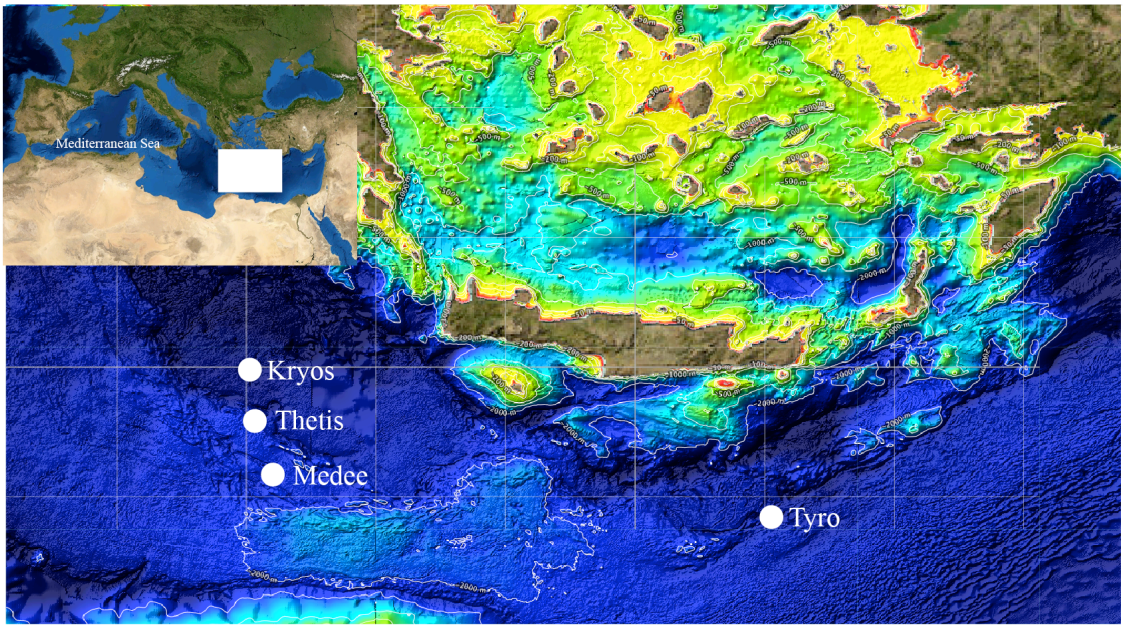

Fig. 1. Location of sampling sites. Data derived from the EMODnet (Marine Observation and Data Network) hydrography portal – http://www.emodnet-hydrography.eu.

regia solution (HNO_3 / HCl, 1 : 3 v/v) and 4 mL of 48 % HF solution containing 2 g of H_3BO_3 added to complex excess HF. Five different aliquots of each standard reference material were digested and analysed. The results are shown in Supplement 1.

DNA, a robust indicator of microbial biomass (Marstorp et al., 2000; Dequiedt et al., 2011), was extracted from sediments using the modified Ranjard et al. (2003) procedure. Sample (0.5 g, dry weight) was frozen in liquid N_2, mixed with 106 mm (700 mg) and 2 mm (150 mg) diameter glass beads, and ground for 1 min at 2000 rpm in a mini bead-beater cell disruptor (Mikro-dismembrator S.B. Braun Biotech International, Melsungen, Germany). The fine powder was resuspended in 1.5 mL of a pre-warmed (70 °C) lysis solution containing 100 mM Tris-HCl (pH 8.0), 100 mM EDTA (pH 8.0), 100 mM NaCl, and 2 % (w/v) SDS (10 mL conical tube), incubated in a hybridisation oven with continuous gentle rotation for 30 min at 70 °C, and then centrifuged at 7000 g for 5 min at 10 °C. Supernatants were recovered, precipitated in 1 / 10 volume of 3 M CH_3COOK (pH 5.5) and one volume of ice-cold isopropanol, then centrifuged at 14 000 rpm for 5 min. The nucleic acids (pellet) were washed with 70 % ethanol and resuspended in 80 µL of sterile ultrapure water. Each extraction was repeated in triplicate.

The purified DNA extract was fluorometrically quantified using Qubit® 2.0 (Life Technologies Corporation, Carlsbad, USA) following the manufacturer's instruction. Extracted DNA was electrophoresed on 0.7 % agarose and compared to serial dilutions of salmon sperm DNA solution (Life Technologies Corporation, Carlsbad, USA) to estimate the DNA concentration. Images of the agarose gels stained with SYBR® Safe (Life Technologies Corporation, Carlsbad, USA) were captured using the VersaDoc system and the Quantity One software (Bio-Rad Laboratories, Hercules, CA, USA) used for densitometric analysis.

3 Results

3.1 Mineralogy

X-ray analyses showed a homogenous mineralogical composition in the sites investigated (Supplement 2) where calcite, magnesium calcite, dolomite, and quartz were identified in all samples. Soluble mineral salts (halite and bischofite) were preserved only in sediments from the Medee and Tyro basins, while they were removed from the Thetis and Kryos sediments during the manipulation procedure in order to investigate the composition of the remaining sediment fraction.

XRD analysis showed that the calcite $d_{(104)}$ peak had a significant asymmetry indicating the possible presence of different calcite generations (Milliman et al., 1971): (i) calcite with a $d_{(104)}$ close to 3.030 Å, (ii) low-Mg calcite with $d_{(104)}$ values close to 3.013 Å, which correspond to a $MgCO_3$ molar content near 8 %; and (iii) high-Mg calcite with $d_{(104)}$ values close to 3.001 Å, which correspond to a $MgCO_3$ molar content near 12 %. The XRD results were in agreement with the SEM determinations, which showed the presence of significant detritic bioclasts (Fig. 2a, b), carbonate lithic fragments (Fig. 2c), and gypsum crystals (Fig. 2d) which originated

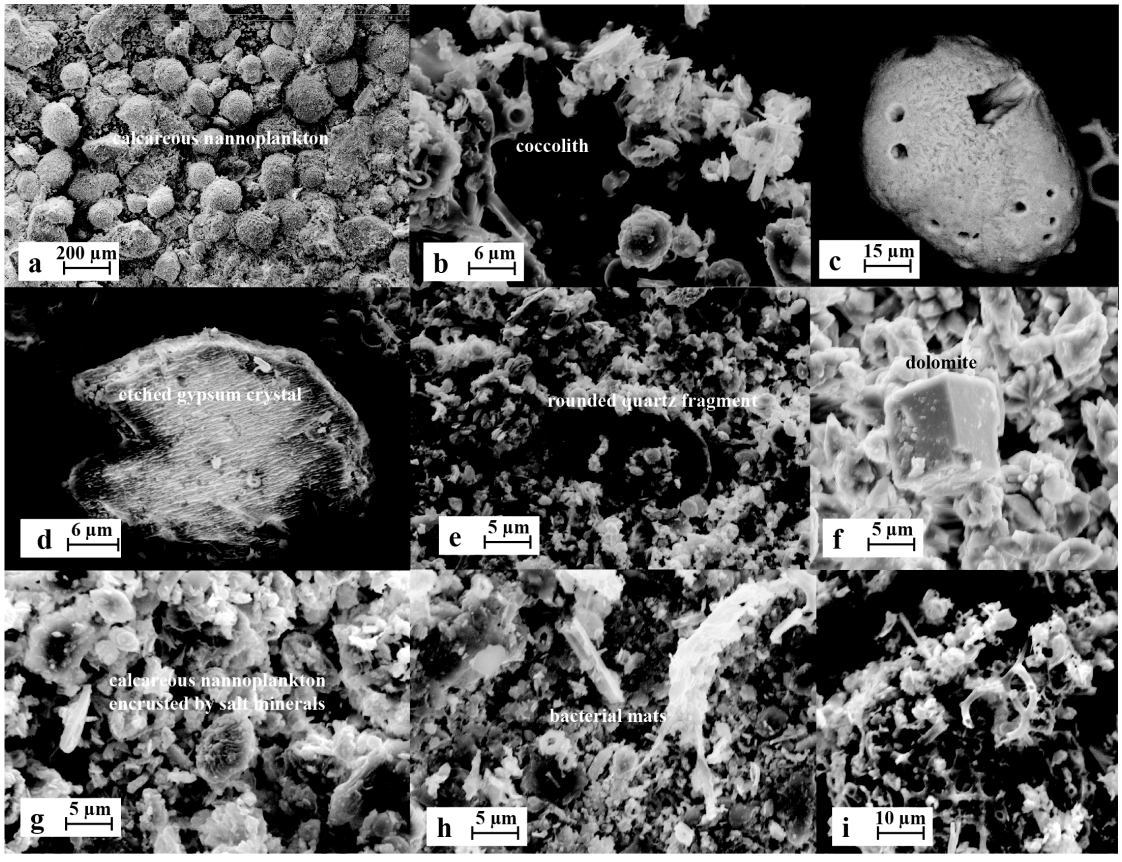

Fig. 2. SEM observations of studied sediments: **(a)** detrital carbonate fraction formed by calcareous nannoplankton; **(b)** possible effects of microbial activity in sediments; **(c)** Mg-free detrital calcite, probably from the "Calcare di Base" formation of Messinian age (see typical cubic crystal ghost of halite); **(d)** etched gypsum crystal showing dissolution figures; **(e)** rounder quartz grain, probably of aeolic origin, enclosed in fine-grained sediment; **(f)** fine-rhombohedral dolomite in fine-grained sediment; **(f)** authigenic salt minerals encrusting detrital nannoplankton; **(h)** possible "organic" textures in sediment; **(i)** possible "organic" textures in sediment and associated bioclastic materials.

from evaporitic Miocene terrains, as well as rounded quartz (Fig. 2e). Authigenic carbonates mainly consisted of high-Mg calcite and dolomite (Fig. 2f), which occasionally contained Fe and magnesium calcite microcrysts.

Soluble salt minerals consisting of halite and bischofite crystals characterised the shallowest sediment layers and appeared often as a crust on the bioclasts (Fig. 2g). Figure 2h and i show the presence of fibrous materials suggesting the presence of microbial mat / organic fractions in the sediments (Fig. 2h, i), as observed by Daffonchio et al., 2006; Rimoldi and Cita, 2007; Ferrer et al., 2012; Stock et al, 2012).

In sediments from the Medee Basin (down to a depth of about 28 cm), detritic minerals (calcite, low-Mg bioclastic calcite, and quartz) represented 50 % of the fraction, decreasing to $\sim$ 40 % in deeper samples. Elevated contents of low-Mg calcite (of bioclastic origin) were also found in the Thetis specimens, whereas these materials were scarce in the Kryos samples, in which more abundant biogenic quartz was found. In the Tyro samples, the amounts of detritic minerals were lower when compared to the other areas (about 40 %), especially in samples from depths of 4–6 and 10–11 cm, where halides, high-Mg calcite, and dolomite were more abundant.

3.2 Molecular microbial biomass in sediments

The amount of DNA recovered from the Tyro sediments ranged from 1.10 to 5.60 ppm (µg DNA per gram of dry sediment) with a mean value of 3.03 ppm. Sediments from the Kryos Basin yielded DNA concentrations which ranged from 2.29 to 4.58 ppm with a mean value of 2.96 ppm. Samples of Medee sediments showed the highest DNA content at 3.46 to 7.34 ppm with an average value of 4.68 ppm. Conversely, sediments from the Thetis site yielded the lowest DNA concentration (mean recovery corresponding to 0.83), with a total DNA content ranging from 0.34 to 1.81 ppm.

3.3 Geochemistry

The concentrations of REE, Zr, and Hf measured in the sediments are reported in Supplement 2. The REE, Zr, and Hf distributions and absolute contents in the sediments

differed between the WS fraction from Tyro/Medee and the FWSS fraction from Kryos/Thetis, where Tyro/Medee had REE concentrations one order of magnitude higher than Kryos/Thetis. In the Tyro and Medee samples, REE values were 70 ± 7.9 and 72.6 ± 7.9 ppm, respectively. The mean content of Zr and Hf ranged between 46.28 ± 9.7 and 47.25 ± 9 ppm and between 0.89 ± 0.17 and 1.05 ± 0.15 ppm, respectively, in Tyro and Medee samples. In the Kryos and Thetis samples, REE concentrations ranged from 32.55 ± 3.7 to 45.2 ± 7.7 ppm, Zr values were 7.33 ± 1.2 to 9.32 ± 2.5 ppm and Hf values were 0.35 ± 0.08 ppm. The higher REE content found in WS sediment fractions (Tyro and Medee basins) with respect to FWSS fractions (Kryos and Thetis basins) suggested that halides and organic matter were preserved in the WS fraction, but removed elsewhere.

In FWSS, a sediment fraction with lower biomass content was found. This may be a consequence of the removal of biological materials caused by the manipulation procedures. Moreover, features of shale-normalised REE patterns versus post-Archean Australian shale (PAAS; Taylor and McLennan, 1995) were different in the Tyro and Medee sediments with respect to the Kryos and Thetis samples (Fig. 3). In Tyro and Medee sediments, shale-normalised patterns showed the typical enrichment in middle REE (MREE); in Kryos and Thetis it is replaced by the positive Gd anomaly. The observed MREE enrichment suggests that MREE fractionation can occur in the investigated sediment assemblage, or that MREE are preferentially scavenged onto sediment surfaces during fluid circulations (Bau, 1999; Hannigan and Sholkovitz, 2001; Haley et al., 2004; Herwartz et al., 2013). The formation of authigenic minerals may thus produce the preferential incorporation of MREE into crystal lattice.

The different REE distributions observed in WS and FWSS sediment fractions were depicted in terms of La / Gd and Gd / Yb shale-normalised values. WS sediment samples were characterised by higher La / Gd and lower Gd / Yb values with respect to the FWSS samples (Fig. 4). The Gd / Yb values in the FWSS samples were due to the occurrence of the above-mentioned positive Gd anomaly that was calculated by the following equation (Moller et al., 2007):

$$\frac{\mathrm{Gd}}{\mathrm{Gd}^*} = \frac{\mathrm{Gd}_n \sqrt{\mathrm{Ho}_n}}{\sqrt{\mathrm{Tb}_n^3}}; \quad (1)$$

Gd / Gd* values are reported in Supplement 3.

A further distinctive characteristic of the REE distribution was the slight positive Ce anomaly observed only in the Kryos sediments ($1.10 \leq \mathrm{Ce/Ce}^* \leq 1.18$), which was not observed in sediments from the Tyro and Medee basins (Fig. 3). This may correspond to that fact that Eh–pH conditions in Tyro and Medee did not allow for the oxidative scavenging of Ce^{3+} to insoluble CeO_2.

The Y / Ho value found in the sediments was between 30 and 55 (molar ratio), whereas the Zr / Hf ratios were between

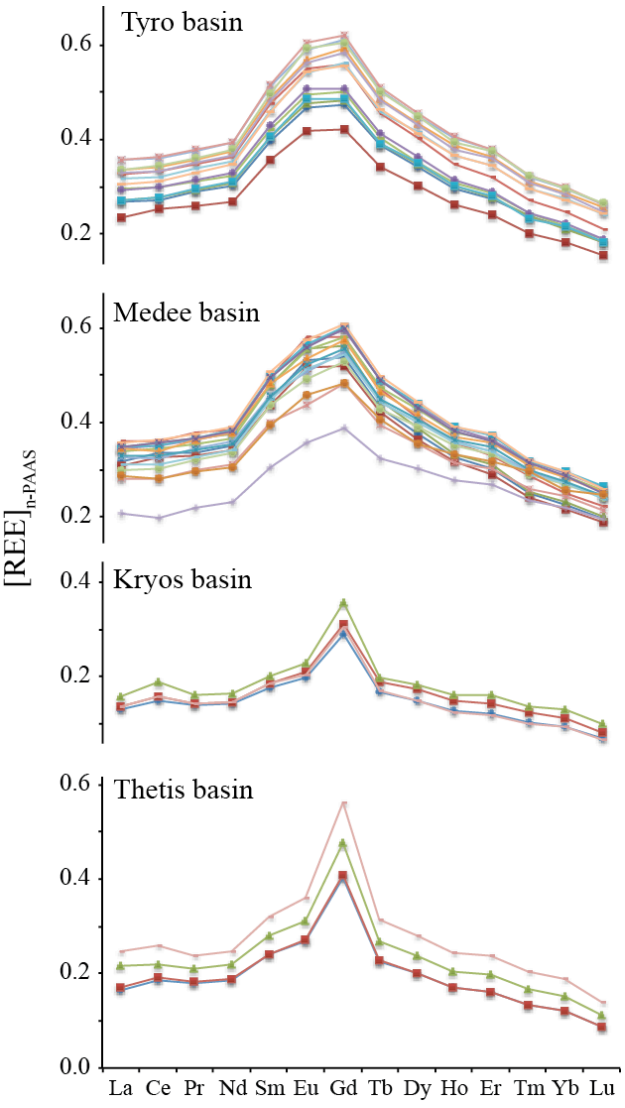

Fig. 3. Shale-normalised REE patterns of the analysed sediments from different basins. Analyses of sediments from the Tyro and Medee basins were carried out on the WS fraction, whereas analyses of sediments from the Kryos and Thetis basins were carried out on the FWSS fraction. For further information, see the text.

40 and 120 (molar ratio). Figure 5 shows that sediments from the Tyro Basin had a broader distribution of Y / Ho and Zr / Hf values. The Y / Ho ratio was always chondritic-subchondritic, whereas the Zr / Hf ratio ranged from superchondritic to subchondritic values. Sediments from the Medee Basin had a narrow distribution of Y / Ho and Zr / Hf values, and the Y / Ho ratio was clustered from slight subchondritic to chondritic values, whereas Zr / Hf was always superchondritic. Also, sediments from the Kryos basins indicated a broader distribution of Y / Ho and Zr / Hf values, which was similar to those from Tyro. Both Y / Ho and Zr / Hf values were always subchondritic in the Kryos sediments. In

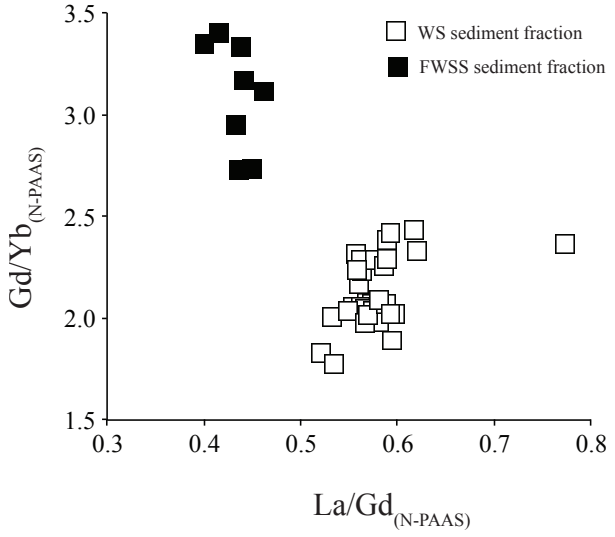

Fig. 4. Features of shale-normalised REE patterns allowing for discriminating between WS and FWSS sediment fractions recognised in terms of La / Gd vs. Gd / Yb normalised ratios.

Thetis sediments, Y / Ho and Zr / Hf behaved similarly even if their distributions fell in a narrow superchondritic range.

The differences observed in terms of REE distributions, amplitudes Gd amplitude anomaly Y / Ho and Zr / Hf values could result from the presence of the detritic fraction and authigenic minerals in the mineral assemblages. In the detritic fraction, REE distribution had a shale-like feature, with Gd / Gd* close to 1, and chondritic signature with Y / Ho and Zr / Hf values of 52 and 71, respectively, inherited from the conditions occurring during the primary crystallisation of these minerals. However, positive Gd anomalies could be considered typical features of bioclastic carbonate fractions, since biogenic carbonates inherit Gd / Gd*>1 values from seawater (Wynhdam et al., 2004; Haley et al., 2005; Azmy et al., 2011), where the positive Gd anomaly is a common feature (De Baar et al., 1985; Alibo and Nozaki, 1999). In sulfates and other minerals formed in marine environments, a positive Gd anomaly is considered a common character of REE distributions (Ehya, 2012, and references therein).

However, REE distributions and the Y–Ho and Zr–Hf relationships in authigenic minerals should provide evidence for the incorporation of these elements into the crystal lattice of authigenic minerals and their concurrent fractionations during competition between dissolved complexation and surface complexation onto these newly formed mineral surfaces (Zhong and Mucci, 1995). In order to identify whether the content of detritic and authigenic carbonates can influence the observed geochemical character of the studied sediments in terms of the Y / Ho and Zr / Hf values, bioclastic calcites and authigenic magnesium carbonate content were compared. Figure 5 shows that Y / Ho and Zr / Hf ratios were inversely related to authigenic magnesium carbonate content in the WS and FWSS fractions, suggesting that the formation of authigenic carbonates involves Y–Ho and Zr–Hf decoupling and preferential Ho and Hf fractionations in the solid phase. The lack of correlation between these ratios and the contents of bioclastic carbonates could be a consequence of the biological mediation of the precipitation of biogenic carbonates (Haley et al., 2005).

Since WS sediment fractions showed MREE enrichments and different Y / Ho and Zr / Hf signatures compared to FWSS, these values were compared to biomass and halide content in sedimentary assemblages in order to evaluate whether the observed geochemical signature was induced by authigenic chloride minerals or by the biological materials in the sediments. Figure 6 shows a significant relationship ($r_{xy} > r_{2.5\%}$) among Zr / Hf, Y / Ho, and the biomass contents, mainly in WS sediment fractions, while a direct relationship between with the amplitude of MREE enrichment (calculated as a MREE / LREE shale-normalised ratio) and biomass contents was less significant ($r_{xy} > r_{20\%}$). However, MREE enrichment was significantly correlated with the halide content in WS ($r_{xy} > r_{2.5\%}$), suggesting the observed MREE-bulged distribution in Tyro and Medee (Fig. 3) was also influenced by the halide crystallisation. The content of these minerals in WS sediments was inversely related to the Y / Ho and Zr / Hf ratios, indicating that the formation of these minerals influenced the behaviour of the Zr–Hf and Y–Ho pairs.

The results reported in this study suggest that the biological component and salt minerals can contain significant REE, Zr, and Hf concentrations. Both biological and authigenic mineral surfaces may fractionate MREE along the REE series and contribute to the Zr–Hf decoupling. Conversely, during these interactions with dissolved-phase Y and Ho behave similarly and their observed fractionation was apparently influenced by the Mg-rich carbonate formation.

4 Discussion

The study of hypersaline deep-sea sediments in the Mediterranean Sea provided the opportunity to determine the behaviour of REE, Zr, and Hf in a large-scale closed natural system, where the effects induced by authigenic minerals, the presence of a detritic sediment fractions, and microbial colonies in the sedimentary assemblages could be distinguished. Although these assemblages belong to very extreme earth environments, recent findings show the presence of several microbial communities, such as prokaryotic and eukaryotic colonies (van der Wielen et al., 2005; 2007; Ferrer et al., 2012), which may provide biological membranes able to scavenge dissolved metals (Rodionov et al., 2006; Erkens et al., 2012). Their membranes generally consist of polysaccharides that can be coated by biofilms of extracellular polymeric substance (EPS) produced by organisms (Domozych et al., 2009). These films play a key role in protecting

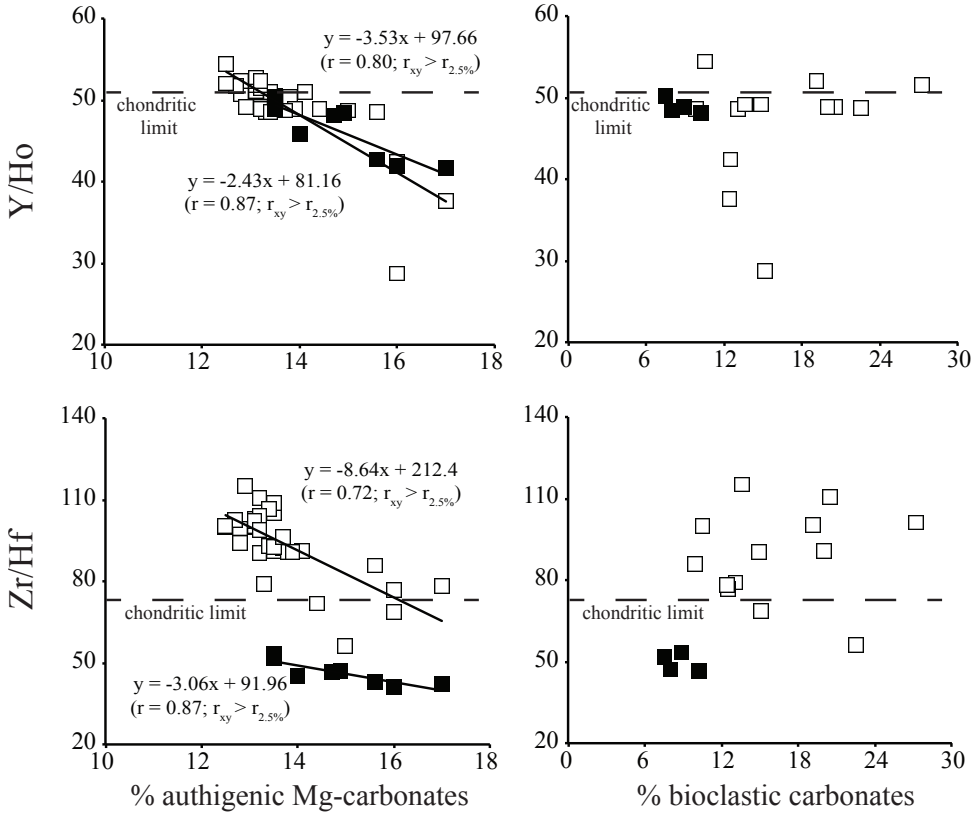

Fig. 5. Relationships between Y / Ho and Zr /,Hf molar values and contents (weight %) of authigenic Mg-rich (dolomite and magnesium calcite) and bioclastic carbonates. Symbols as in Fig. 4. Chondritic values are reported for comparison.

the external cellular walls from the surrounding environment (Merroun et al., 1998). Both microbial assemblages and their EPS coatings occur in a wide spectrum of environmental conditions. Under these conditions, microbial assemblages in sediments may fractionate trace metals during the complex sediment–water interface processes (Monji et al., 2008; Censi et al., 2013).

In FWSS samples collected from Thetis and Kryos seafloor basins, lower trace element concentrations, positive Gd anomalies, and subchondritic Y / Ho and Zr / Hf values were seen. As these were the residues remaining after the removal of water-soluble minerals and biological materials from sedimentary assemblages, they were primarily composed of detritic minerals, bioclastic products (quartz, carbonate fragments, gypsum, foraminifera shells, coccoliths, radiolaria), and authigenic Mg-rich carbonates in the FWSS sediment fractions. The Gd anomaly does not occur in quartz and other detritic minerals (Bach et al., 2003; Goetze et al., 2004; Xie et al., 2005), whereas a positive Gd anomaly is recorded in marine carbonates, such as those present in chemical sediments and during the deposition of stromatolites (Haley et al., 2005; Bau and Alexander, 2006; Mastandrea et al., 2010; Army et al., 2011; Ehya, 2012; Corkeron et al., 2012).

The capacity for REE^{3+} to act as a substitute for Ca^{2+} in several carbonate minerals, including calcite (Zhong and Mucci, 1995), is related to the similarity of the ionic radius between Ca^{2+} and REE^{3+} in six-fold coordination, driving the Ca–REE substitution in the crystal lattice of trigonal carbonates. Since the Ca^{2+} ionic radius is close to 1.00 Å, whereas ionic dimensions of Eu^{3+} and its REE neighbours are close to 0.95 Å (Shannon, 1976), the Eu–Ca substitution should be preferred, as reported by Terakado and Masuda (1988). However, if carbonate precipitation occurs in hypersaline deep-sea brines under high ionic strength and reducing conditions, Eu should be in the Eu^{2+} form, with a subsequent increase in its solubility favouring the preferential partitioning of other MREEs, from Sm to Tb, during the formation of authigenic carbonates (Bau, 1991, Stipp et al., 2003).

Despite the lack of data for dolomite, laboratory experiments on $CaCO_3$ crystallisation (both calcite and aragonite) indicate the preferential incorporation of Ho into $CaCO_3$ with respect to Y (Qu et al., 2009), implying a potential subchondritic Y / Ho signature for these minerals. Tanaka et al. (2004, 2008) found a preferential Y enrichment in the dissolved phase during calcite crystallisation with respect to Ho, interpreted as a Ho–CO_3 and Y–CO_3 bonding difference in carbonate minerals. The preferential Y–Ho decoupling

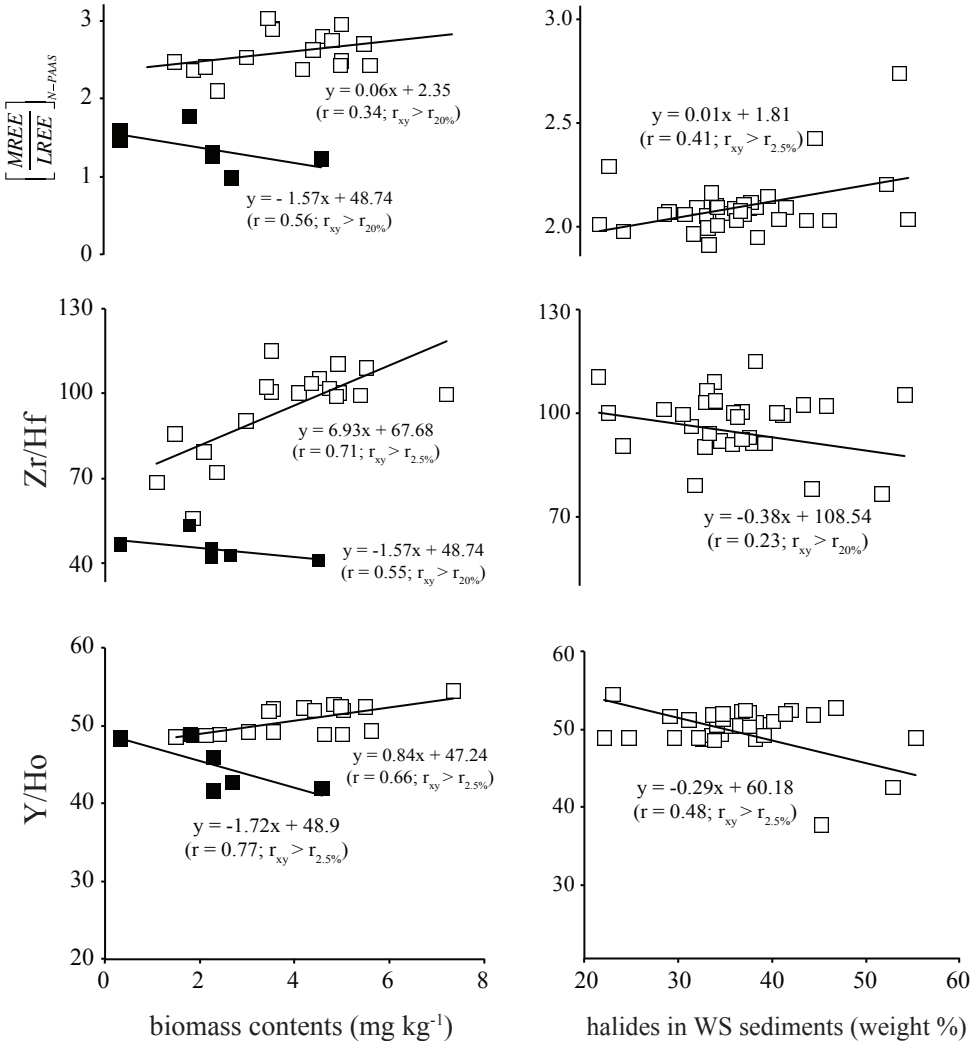

Fig. 6. Relationships between amplitudes of MREE enrichment (in terms of MREE / LREE normalised concentrations), Y / Ho and Zr / Hf molar ratios and biomass (mg kg^{-1}) and halide contents (weight %) in studied assemblages. Tests of significance for observed distributions have been carried out measuring the $t_{a/2}$ Student factor. $r_{xy} > r_{\mathrm{nm}\%}$ indicates that the measured sampling correlation factor r_{xy} is greater than the appropriate t_{n-2} degree of freedom. Symbols as in Fig. 4.

during carbonate crystallisation was found in the samples from this study (Fig. 5) and explained the observed subchondritic Y / Ho values found in sediments with high magnesium carbonate contents. The subchondritic value observed for the Zr / Hf ratio found in the sediment fractions suggested that Y / Ho and Zr / Hf behaved similarly during the crystallisation of authigenic magnesium carbonates. A possible explanation for the observed subchondritic Zr / Hf signature of FWSS sediment fractions from the Kryos and Thetis basins can be found in the simplified electrostatic model proposed by Bau and Koschinsky (2009). These authors proposed the dissolved speciation of elements and surface charge of potentially sorbent species could lead to elemental fractionation during sorption. In hypersaline brines from the Mediterranean Sea, slight acidic conditions are found (De Lange et al., 1990) and PHREEQC calculations simulating these environmental conditions suggested that Zr and Hf speciation were dominated by $[Zr(OH)_4]^0$ and $[Hf(OH)_5]^-$ complexes in brines. Since the surfaces of carbonates crystallising from brines at pH < 8 are positively charged (Pokrovsky et al., 1999; Pokrovsky and Schott (1999), a preferential scavenging of $[Hf(OH)_5]^-$ with respect to $[Zr(OH)_4]^0$ was expected as a consequence of the authigenic magnesium carbonates' crystallisation.

WS sediment fractions from the Tyro and Medee sites were MREE-enriched, together with chondritic and superchondritic Y / Ho and Zr / Hf values. In these sediments, authigenic carbonates and detritic phases were associated with soluble salts with evidence of microbial communities (Supplement 2, 3). As previously mentioned, MREE-bulge

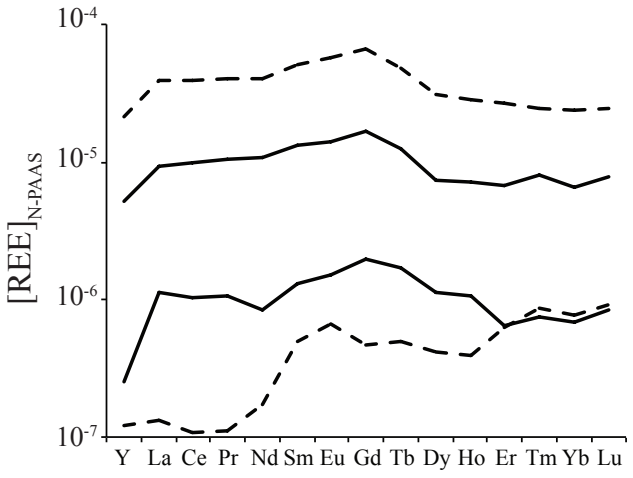

Fig. 7. Shale-normalised REE distributions in selected kainite ($MgSO_4{\cdot}KCl{\cdot}3H_2O$) (dashed curves) and sylvite (KCl) (solid curves) samples. Data from Ragusa (2013).

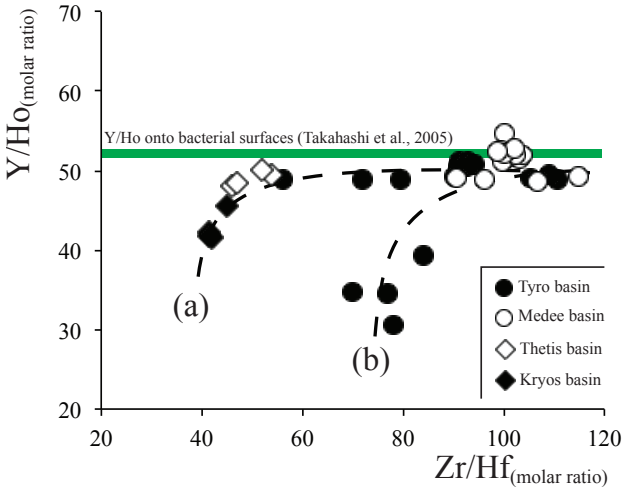

Fig. 8. Y / Ho vs. Zr / Hf behaviour. **(a)** and **(b)**: trends represent hypothetical mixing arrays as detailed in the text. The range of Y / Ho values measured onto bacterial surfaces by Takahashi et al. (2005) is reported for reference.

distributions in shale-normalised REE patterns from sediments may result from the presence of iron oxyhydroxide or phosphates in the mineral assemblage. However, these minerals were not found in the study sediments from the deep-sea Mediterranean basins. On the other hand, the linear relationship found between the amplitude of MREE enrichments (in terms of shale-normalised MREE / LREE ratio) and halide content in WS sediment fractions (Fig. 6) suggested a preferential MREE fractionation during the deposition of authigenic halide. This was in agreement with the results of Steinmann and Stille (2001), as well as the recent REE analyses of soluble sulfates and chlorides from undisturbed Messinian evaporitic sequences from Sicily showing MREE-bulge distributions (Ragusa, 2013) (Fig. 7). MREE-bulge distribution was also typical of REE fractionation between biological surfaces and the dissolved phase, explained by MREE preferentially binding to carboxylate groups of soft organic matter (Takahashi et al., 2010).

The lack of Zr / Hf, and the inverse relationship between Y / Ho and halide content (Fig. 6) implied that chondritic Y / Ho and superchondritic Zr / Hf values cannot simply be explained in terms of halide content in the WS sediment. However, the distributions observed for Zr / Hf and Y / Ho ratios with respect to the microbial community levels measured in terms of biomass content (Fig. 6) suggested that Zr–Hf and Y–Ho fractions in the sediments could be influenced by microbiological activity. If the DNA content was low, its effect on the Y–Ho and Zr–Hf fractionations became negligible, which was in agreement with the inverse Y / Ho and Zr / Hf vs. biomass content found in FWSS sediment fractions (Fig. 6). In samples with higher DNA content, larger microbial communities were expected with larger Zr–Hf fractionations, as was observed in the WS sediments. These features were also consistent with the simplified electrostatic model proposed by Bau and Koschinsky (2009) applied to the dissolved Zr and Hf speciation in brine. In fact, Eubacteria and Archaea, including the phylotypes identified by La Cono et al. (2009) and Ferrer et al. (2012), synthesise a plethora of glycoconjugates and polysaccharides with important structural and functional roles. These peptidoglycans and glycoproteins coat the external layers of bacteria and Archaea, respectively, reinforcing the cytoplasmic membranes and providing binding sites for dissolved metal ion complexes that have negative surface charges (Rendueles et al., 2013). Therefore, $[Zr(OH)_4]^0$ was preferentially scavenged by biological surfaces with respect to the anionic $[Hf(OH)_5]^-$ complex, which explained the observed Zr / Hf superchondritic signature in sediments richer in biomass. Moreover, this scenario was also consistent with lab experiments on biomass sorption of dissolved Zr and Hf under acidic conditions, where the preferential Zr scavenging with respect to Hf is seen (Monji et al., 2008).

Since the dominant dissolved Y and Ho complexes in brines were $[YCl]^{2+}$ and $[HoCl]^{2+}$, respectively, Y–Ho decoupling was not expected as a consequence of interactions with negatively charged biological membranes and films based upon the simplified electrostatic model (Bau and Koschinsky, 2009). Therefore, a chondritic Y / Ho signature in samples where DNA content was higher can be justified. The observed lack of fractionation between Y and Ho was also in agreement with experimental data from Takahashi et al. (2005) obtained during scavenging processes involving bacterial surfaces. Variations in the Zr / Hf and Y / Ho ratios in FWSS sediment fractions, where biomass was partially removed, were probably due to the overwhelming concurrent presence of authigenic Mg-rich carbonates that preferentially scavenged Ho and Hf from the dissolved fraction.

These data suggested that Y / Ho and Zr / Hf ratios were sensitive to changes in the mineralogical composition and biomass content in authigenic sediment fractions and could indicate mixing processes among microbial assemblages, chemical marine sediments, and Mg-rich carbonates in different proportions. If halide was removed, Y / Ho and Zr / Hf values could evolve along the "a" path, otherwise they would follow trend "b". In any case, comparison of concurrent Y–Ho and Zr–Hf fractionations to the "chondritic" signatures of their ratios appeared to be a suitable proxy indicator of microbial activity in sedimentary assemblages.

5 Conclusions

Tectonic settling of the seafloor in the eastern Mediterranean led to deep-sea basins filled with reducing hypersaline brines, extreme environments where the occurrence of authigenic minerals (Mg-rich carbonates and halides) and microbial colonies in the sedimentary assemblages influenced the geochemical distribution of REE, Zr, and Hf. Geochemical determination of authigenic and detritic sediment fractions showed MREE enrichments, a positive Gd anomaly, and Y / Ho and Zr / Hf molar ratios spanning a wide range of values. MREE enrichment was interpreted as governed by the presence of soluble halides in Tyro and Medee sediments.

Our results show that the reciprocal Zr-Hf and Y-Ho behaviour is influenced by their dissolved speciations at the brine–sediment interface. The Zr–Hf fractionation without Y-Ho partitioning is observed when the higher microbial activity (DNA content) in sediments occurs. When this activity is low or absent, both Zr and Y are partitioned compared with Hf and Ho, respectively. Therefore, the Zr-Hf decoupling and the concurrent absence of an analogous Y-Ho partitioning can be considered as a promising new geochemical tool to recognise traces of microbial activity in sedimentary assemblages. The crystallisation of authigenic halide does not significantly fractionate Zr and Hf, but can be responsible for the MREE enrichment in sedimentary assemblages.

On the other hand, the halides' formation does not involve Zr–Hf fractionations compared to the chondritic values but allows for MREE partitioning. Therefore, a geochemical investigation focused on the REE distributions and the reciprocal fractionations of Y–Ho and Zr–Hf pairs can represent a suitable tool to discriminate among authigenic fraction, detritic minerals, and evidence of microbial activity in marine sediments.

Supplementary material related to this article is available online at http://www.biogeosciences.net/11/1125/2014/bg-11-1125-2014-supplement.pdf.

Acknowledgements. We are indebted to M. Yakimov and his team for facilities offered during the Mamba 2010 oceanographic cruise and to G. Tranchida, E. Oliveri, and M. Sprovieri, who allowed us to investigate sediment samples collected during the cruise. The bathymetric metadata and digital terrain model data products used in Fig. 1 have been derived from the EMODnet (Marine Observation and Data Network) hydrography portal – http://www.emodnet-hydrography.eu. The authors are also very grateful to Ignacio Gonzalez-Alvarez, to an anonymous reviewer, and to Filip Meysman (AE) for their careful and dedicated job of critical revision of the first version of the manuscript. Special thanks also need to be extended to Alessandro Incarbona for his critical reading of the manuscript.

Edited by: F. Meysman

References

Alibo, D. S. and Nozaki, Y.: Rare earth elements in seawater: Particle association, shale-normalization, and Ce oxidation, Geochim. Cosmochim. Acta, 63, 363–372, 1999.

Andrianov, A. V., Savel'Eva, O. A., Bauer, E., and Staunton, J. B.: Squeezing the crystalline lattice of the heavy rare-earth metals to change their magnetic order: Experiment and ab initio theory, Phys. Rev. B, 84, 2011.

Azmy, K., Brand, U., Sylvester, P., Gleeson, S. A., Logan, A., and Bitner, M. A.: Biogenic and abiogenic low-Mg calcite (bLMC and aLMC): Evaluation of seawater-REE composition, water masses and carbonate diagenesis, Chem. Geol., 280, 180–190, 2011.

Bach, W., Roberts, S., Vanko, D. A., Binns, R. A., Yeats, C. J., Craddock, P. R., and Humphris, S. E.: Controls of fluid chemistry and complexation on rare-earth element contents of anhydrite from the Pacmanus subseafloor hydrothermal system, Manus Basin, Papua New Guinea, Miner Deposita, 38, 916–935, 2003.

Bau, M.: Rare-earth element mobility during hydrothermal and metamorphic fluid-rock interaction and the significance of the oxidation state of europium, Chem. Geol, 93, 219–230, 1991.

Bau, M.: Scavenging of dissolved yttrium and rare earths by precipitating iron oxyhydroxide: Experimental evidence for Ce oxidation, Y-Ho fractionation, and lanthanide tetrad effect, Geochim. Cosmochim. Acta, 63, 67–77, 1999.

Bau, M. and Alexander, B.: Preservation of primary REE patterns without Ce anomaly during dolomitization of Mid-Paleoproterozoic limestone and the potential re-establishment of marine anoxia immediately after the "Great Oxidation Event", S. Afr. J. Geol., 109, 81–86, 2006.

Bau, M. and Koschinsky, A.: Oxidative scavenging of cerium on hydrous Fe oxide: Evidence from the distribution of rare earth elements and yttrium between Fe oxides and Mn oxides in hydrogenetic ferromanganese crusts, Geochem. J., 43, 37–47, 2009.

Bortoluzzi, G., Borghini, M., La Cono, V., Genovese, L., Foraci, F., Polonia, A., Riminucci, F., Marozzi, G., and Yakimov, M.: The exploration of deep anoxic basins of the earstern Mediterranean sea, Marine Reasearch at CNR, 2011.

Camerlenghi, A.: Anoxic basins of the eastern Mediterranean: geological framework, Mar. Chem., 31, 1–19, 1990.

Censi, P., Cangemi, M., Brusca, L., Madonia, P., Saiano, F., and Zuddas, P.: The behavior of rare-earth elements, Zr and Hf during biologically-mediated deposition of silica-stromatolites and carbonate-rich microbial mats, Gondwana Research, 2013.

Cita, M. B.: Exhumation of Messinian evaporites in the deep-sea and creation of deep anoxic brine-filled collapsed basins, Sed. Geol., 188, 357–378, 2006.

Corkeron, M., Webb, G. E., Moulds, J., and Grey, K.: Discriminating stromatolite formation modes using rare earth element geochemistry: Trapping and binding versus in situ precipitation of stromatolites from the Neoproterozoic Bitter Springs Formation, Northern Territory, Australia, Precambrian Res, 212–213, 194–206, 2012.

Daffonchio, D., Borin, S., Brusa, T., Brusetti, L., Van Der Wielen, P. W. J. J., Bolhuis, H., Yakimov, M. M., D'Auria, G., Giuliano, L., Marty, D., Tamburini, C., McGenity, T. J., Hallsworth, J. E., Sass, A. M., Timmis, K. N., Tselepides, A., De Lange, G. J., Hübner, A., Thomson, J., Varnavas, S. P., Gasparoni, F., Gerber, H. W., Malinverno, E., Corselli, C., Garcin, J., McKew, B., Golyshin, P. N., Lampadariou, N., Polymenakou, P., Calore, D., Cenedese, S., Zanon, F., and Hoog, S.: Stratified prokaryote network in the oxic-anoxic transition of a deep-sea halocline, Nature, 440, 203–207, 2006.

de Baar, H. J. W., Brewer, P. G., and Bacon, M. P.: Anomalies in rare earth distributions in seawater: Gd and Tb, Geochim. Cosmochim. Acta, 49, 1961–1969, 1985.

De Lange, G. J., Middelburg, J. J., Van der Weijden, C. H., Catalano, G., Luther Iii, G. W., Hydes, D. J., Woittiez, J. R. W., and Klinkhammer, G. P.: Composition of anoxic hypersaline brines in the Tyro and Bannock Basins, eastern Mediterranean, Mar. Chem., 31, 63–88, 1990.

Dequiedt, S., Saby, N. P. A., Lelievre, M., Jolivet, C., Thioulouse, J., Toutain, B., Arrouays, D., Bispo, A., Lemanceau, P., and Ranjard, L.: Biogeographical patterns of soil molecular microbial biomass as in?uenced by soil characteristics and management, Glob Ecol Biogeogr., 20, 641–652, 2011.

Domozych, D. S., Wilson, R., and Domozych, C. R.: Photosynthetic eukaryotes of freshwater wetland biofilms: Adaptations and structural characteristics of the extracellular matrix in the green alga, cosmarium reniforme (zygnematophyceae, streptophyta), J. Eukaryot. Microbiol., 56, 314–322, 2009.

Du, X. and Graedel, T. E.: Uncovering the end uses of the rare earth elements, Science of the Total Environment, 461–462, 781–784, 2013.

Ehya, F.: Rare earth element and stable isotope (O, S) geochemistry of barite from the Bijgan deposit, Markazi Province, Iran, Mineral. Petrol., 104, 81–93, 2012.

Erkens, G. B., Majsnerowska, M., Ter Beek, J., and Slotboom, D. J.: Energy coupling factor-type ABC transporters for vitamin uptake in prokaryotes, Biochemistry-Us, 51, 4390–4396, 2012.

Ferrer, M., Werner, J., Chernikova, T. N., Bargiela, R., Fernández, L., La Cono, V., Waldmann, J., Teeling, H., Golyshina, O. V., Glöckner, F. O., Yakimov, M. M., and Golyshin, P. N.: Unveiling microbial life in the new deep-sea hypersaline Lake Thetis, Part II: A metagenomic study, Environ. Microbiol., 14, 268–281, 2012.

Goetze, J., Ploetze, M., Graupner, T., Hallbauer, D. K., and Bray, C. J.: Trace element incorporation into quartz: A combined study by ICP-MS, electron spin resonance, cathodoluminescence, capillary ion analysis, and gas chromatography, Geochim. Cosmochim. Acta, 68, 3741–3759, 2004.

Govindaraiu, K.: Compilation of working values and sample description for 170 international reference samples of mainly silicate rocks and minerals, Geostandard newsletter 7, 3–226, 1984.

Haley, B. A., Klinkhammer, G. P., and McManus, J.: Rare earth elements in pore waters of marine sediments, Geochim. Cosmochim. Acta, 68, 1265–1279, 2004.

Haley, B. A., Klinkhammer, G. P., and Mix, A. C.: Revisiting the rare earth elements in foraminiferal tests, Earth Plan. Sci. Lett., 239, 79–97, 2005.

Hannigan, R. E. and Sholkovitz, E. R.: The development of middle rare earth element enrichments in freshwaters: Weathering of phosphate minerals, Chem. Geol., 175, 495–508, 2001.

Hein, J. R., Mizell, K., Koschinsky, A., and Conrad, T. A.: Deep-ocean mineral deposits as a source of critical metals for high- and green-technology applications: Comparison with land-based resources, Ore Geol. Rev., 51, 1–14, 2013.

Herwartz, D., Toetken, T., Jochum, K. P., and Sander, P. M.: Rare earth element systematics of fossil bone revealed by LA-ICPMS analysis, Geochim. Cosmochim. Acta, 103, 161–183, 2013.

Himmler, T., Bach, W., Bohrmann, G., and Peckmann, J.: Rare earth elements in authigenic methane-seep carbonates as tracers for fluid composition during early diagenesis, Chem. Geol., 277, 126–136, 2010.

Hsu, K. J. and Montadert, L., Bernoulli, D., Cita, M. B., Erickson, A., Garrison, R. E., Kidd, R. B., Méliéres, F., Müller, C., and Wright, R. (Editors): Initial Reports DSDP, 42, Part 1. U.S. Government Printing Office, Washington, D.C., 1249 pp, 1978.

La Cono, V., Smedile, F., Bortoluzzi, G., Arcadi, E., Maimone, G., Messina, E., Borghini, M., Oliveri, E., Mazzola, S., L'Haridon, S., Toffin, L., Genovese, L., Ferrer, M., Giuliano, L., Golyshin, P. N., and Yakimov, M. M.: Unveiling microbial life in new deep-sea hypersaline Lake Thetis. Part I: Prokaryotes and environmental settings, Environ. Microbiol., 13, 2250–2268, 2011.

Marstorp, H., Guan, X., and Gong, P.: Relationship between ds-DNA, chloroform labile C and ergosterol in soils of different organic matter contents and pH, Soil Biol. Biochem., 32, 879–882, 2000.

Mastandrea, A., Barca, D., Guido, A., Tosti, F., and Russo, F.: Rare earth element signatures in the Messinian pre-evaporitic Calcare di Base formation (Northern Calabria, Italy): Evidence of normal seawater deposition, Carbonate Evaporite, 25, 133–143, 2010.

Merroun, M. L., Ben Omar, N., Gonzalez-Munoz, M. T., and Arias, J. M.: Myxococcus xanthus biomass as biosorbent for lead, J. Appl. Microbiol., 84, 63–67, 1998.

Milliman, J. D., Gastner, M., and Muller, J.: Utilization of magnesium in coralline algae, Geol. Soc. Am. Bull., 82, 573–580, 1971.

Möller, P. and Dulski, P.: Fractionation of Zr and Hf in cassiterite, Chem. Geol., 40, 1–12, 1983.

Möller, P., Rosenthal, E., Geyer, S., Guttman, J., Dulski, P., Rybakov, M., Zilberbrand, M., Jahnke, C., and Flexer, A.: Hydrochemical processes in the lower Jordan valley and in the Dead Sea area, Chem. Geol., 239, 27–49, 2007.

Monji, A. B., Ahmadi, S. J., and Zolfonoun, E.: Selective biosorption of zirconium and hafnium from acidic aqueous solutions by rice bran, wheat bran and platanus orientalis tree leaves, Separ Sci. Technol., 43, 597–608, 2008.

Moriwaki, H., Koide, R., Yoshikawa, R., Warabino, Y., and Yamamoto, H.: Adsorption of rare earth ions onto the cell walls of wild-type and lipoteichoic acid-defective strains of Bacillus subtilis, Appl. Microbiol. Biotechnol., 97, 3721–3728, 2013.

Pokrovsky, O. S. and Schott, J.: Processes at the magnesium-bearing carbonates/solution interface. II. Kinetics and mechanism of magnesite dissolution, Geochim. Cosmochim. Acta, 63, 881–897, 1999.

Pokrovsky, O. S., Schott, J., and Thomas, F.: Dolomite surface speciation and reactivity in aquatic systems, Geochim. Cosmochim. Acta, 63, 3133–3143, 1999.

Qu, C. L., Liu, G., and Zhao, Y. F.: Experimental study on the fractionation of yttrium from holmium during the coprecipitation with calcium carbonates in seawater solutions, Geochem. J., 43, 403–414, 2009.

Ragusa, E.: Geochemical behaviour of Rare Earths during the crystallization of salt minerals, Thetis, University of Palermo (Italy), 2014.

Ranjard, L., Lejon, D., Mougel, C., Scherer, L., Merdinoglu, D., and Chaussod, R.: Sampling strategy in molecular microbial ecology: in?uence of soil sample size on DNA fingerprinting analysis of fungal and bacterial communities, Environ. Microbiol., 5, 1111–1120, 2003.

Rendueles, O., Kaplan, J. B., and Ghigo, J. M.: Antibiofilm polysaccharides, Environ. Microbiol., 15, 334–346, 2013.

Rimoldi B. and Cita B. M.: Deep sea turbidites in brine-filled anoxic basins of the Mediterranean Ridge, Depositional madels based on sedimentological and geochemical characteriszation, Rend. Fis. Acc. Lincei, 9, 27–47, 2007.

Rimstidt, J. D., Balog, A., and Webb, J.: Distribution of trace elements between carbonate minerals and aqueous solutions, Geochim. Cosmochim. Acta, 62, 1851–1863, 1998.

Rodionov, D. A., Hebbeln, P., Gelfand, M. S., and Eitinger, T.: Comparative and functional genomic analysis of prokaryotic nickel and cobalt uptake transporters: Evidence for a novel group of ATP-binding cassette transporters, J. Bacteriol., 188, 317–327, 2006.

Ryan, W. F. B. and Hsu, K. J.: Initial Reports DSDP, 13, Part 1. U.S. Government Printing Office, Washington, DC, 514 pp., 1973.

Shannon, R. D.: Revised effective ionic radii and systematic studies of interatomic distances in halides and chalcogenides, Acta Crystallogr., B25, 925–946, 1976.

Steinmann, M., Stille, P., Mengel, K., and Kiefel, B.: Trace element and isotopic evidence for REE migration and fractionation in salts next to a basalt dyke, Appl. Geochem., 16, 351–361, 2001.

Stipp, S. L. S., Lakshtanov, L. Z., Jensen, J. T., and Baker, J. A.: Eu^{3+} uptake by calcite: Preliminary results from coprecipitation experiments and observations with surface-sensitive techniques, J. Contam. Hydrol., 61, 33–43, 2003.

Stock, A., Breiner, H. W., Pachiadaki, M., Edgcomb, V., Filker, S., La Cono, V., Yakimov, M. M., and Stoeck, T.: Microbial eukaryote life in the new hypersaline deep-sea basin Thetis, Extremophiles, 16, 21–34, 2012.

Takahashi, Y., Chatellier, X., Hattori, K. H., Kato, K., and Fortin, D.: Adsorption of rare earth elements onto bacterial cell walls and its implication for REE sorption onto natural microbial mats, Chem. Geol., 219, 53–67, 2005.

Takahashi, Y., Hirata, T., Shimizu, H., Ozaki, T., and Fortin, D.: A rare earth element signature of bacteria in natural waters? Chem. Geol., 244, 569–583, 2007.

Takahashi, Y., Yamamoto, M., Yamamoto, Y., and Tanaka, K.: EXAFS study on the cause of enrichment of heavy REEs on bacterial cell surfaces, Geochim. Cosmochim. Acta, 74, 5443–5462, 2010.

Tanaka, K., Ohta, A., and Kawabe, I.: Experimental REE partitioning between calcite and aqueous solution at 25 °C and 1 atm: Constraints on the incorporation of seawater REE into semount-type limestones, Geochem. J., 38, 19–32, 2004.

Tanaka, K., Takahashi, Y., and Shimizu, H.: Local structure of Y and Ho in calcite and its relevance to Y fractionation from Ho in partitioning between calcite and aqueous solution, Chem. Geol., 248, 104–113, 2008.

Taylor, S. R. and McLennan, S. M.: The geochemical evolution of the continental crust, Rev. Geophys., 33, 241–265, 1995.

Terakado, Y. and Masuda, A.: Coprecipitation of Rare-Earth Elements with calcite and aragonite, Chem. Geol. 69, 103–110, 1988.

Tranchida, G., Oliveri, E., Angelone, M., Bellanca, A., Censi, P., D'Elia, M., Neri, R., Placenti, F., Sprovieri, M., and Mazzola, S.: Distribution of rare earth elements in marine sediments from the Strait of Sicily (western Mediterranean Sea): Evidence of phosphogypsum waste contamination, Mar. Pollut. Bull., 62, 182–191, 2011.

Van Der Wielen, P. W. J. J. and Heijs, S. K.: Sulfate-reducing prokaryotic communities in two deep hypersaline anoxic basins in the Eastern Mediterranean deep sea: Brief report, Environ. Microbiol., 9, 1335–1340, 2007.

Van Der Wielen, P. W. J. J., Bolhuis, H., Borin, S., Daffonchio, D., Corselli, C., Giuliano, L., D'Auria, G., De Lange, G. J., Huebner, A., Varnavas, S. P., Thomson, J., Tamburini, C., Marty, D., McGenity, T. J., and Timmis, K. N.: The enigma of prokaryotic life in deep hypersaline anoxic basins, Science, 307, 121–123, 2005.

Xie, X., Ellis, A., Wang, Y., Xie, Z., Duan, M., and Su, C.: Geochemistry of redox-sensitive elements and sulfur isotopes in the high arsenic groundwater system of Datong Basin, China, Sci. Total Environ., 407, 3823–3835, 2009.

Young, R.: The Rietveld Method, International Union of Crystallography, Oxford University Press, Oxford, 1993.

Zhang, F., Xu, H., Konishi, H., Kemp, J. M., Roden, E. E., and Shen, Z.: Dissolved sulfide-catalyzed precipitation of disordered dolomite: Implications for the formation mechanism of sedimentary dolomite, Geochim. Cosmochim. Acta, 97, 148–165, 2012.

Zhong, S. J. and Mucci, A.: Partitioning of Rare-Earth Elements (REEs) between Calcite and Seawater Solutions at 25-Degrees-C and 1 Atm, and High Dissolved Ree Concentrations, Geochim. Cosmochim. Acta, 59, 443–453, 1995.